On the Role of Aerosol Radiative Effect in the Wet Season Onset Timing over the Congo Rainforest during Boreal Autumn.

Sudip Chakraborty[1*], Jonathon H. Jiang[1], Hui Su[1], and Rong Fu[2]

*Corresponding author: Sudip Chakraborty. Sudip.chakraborty@jpl.nasa.gov

1. Jet Propulsion Laboratory, California Institute of Technology, Pasadena, CA, USA
2. Department of Atmospheric and Oceanic Sciences, University of California, Los Angeles

Keywords: Equatorial African Precipitation, dry season length, Wet season onset

Abstract

The boreal summer dry season length is reported to have been increasing in the last three decades over the Congo rainforest, which is the second-largest rainforest in the world. In some years, the wet season in boreal autumn starts early while in others it arrives late. The mechanism behind such a change in wet season onset date has not been investigated yet. Using multi-satellite datasets, we discover that the variation of aerosols in dry season plays a major role in determining the subsequent wet season onset. Dry season aerosol optical depth (AOD) influences the strength of the southern African easterly jet (AEJ-S) and thus the onset of the wet season. Higher AOD associated with a higher dust mass flux reduces the net downward shortwave radiation and decreases the surface temperature over the Congo rainforest region, leading to a stronger meridional temperature gradient between the rainforest and the Kalahari Desert as early as in June. The latter, in turn, strengthens the AEJ-S, sets in an early and a stronger easterly flow, leads to a stronger equatorward convergence and an early onset of the wet season in late August to early September. The mean AOD in the dry season over the region is strongly correlated ($r = 0.7$) with the timing of the subsequent wet season onset. Conversely, in low AOD years, the onset of the wet season over the Congo basin is delayed to mid-October.

1. Introduction

Wet season onset over the Congo rainforest marks the end of the dry season with increasing precipitation; thus it is important for the groundwater as well as soil moisture replenishments, photosynthetic rate, greenness, ecology, and sustainability of the rainforest, especially in a warming climate (Erfanian et al., 2017; Lewis et al., 2011, 2013; Marengo et al., 2008). Recent studies show that the Congo rainforest, which is the second-largest rainforest following the Amazon, has been experiencing a longer boreal summer dry season (Malhi and Wright, 2004; Zhou et al., 2014). The dry season length has increased by 6.4-10.4 days per decade between 1988-2013 and the rainfall is declining at a striking rate of -0.32 ± 0.10 mm/day per decade over the last 50 years (Jiang et al., 2019). Observations also indicate a long-term drying and declining of greenness in the Congo rainforest (Zhou et al., 2014). Annual rainfall over much of the Congo rainforest is marginal to sustain the rainforest (Mayer and Khalyani, 2011; Staver et al., 2011). A significant reduction of rainfall due to the delay of the main rainy season in boreal autumn can lead to significant water stress to the rainforest. Besides, continuous deforestation, droughts, and global warming pose serious threats to the rainforest, make it more vulnerable and unsustainable for future existence (Tyukavina et al., 2018).

Congo basin experiences two different rainy seasons during March-May (MAM) (Nicholson and Dezfuli, 2013) and September-December (SOND) (Dezfuli and Nicholson, 2013) with the twice-annual passage of the intertropical convergence zone (ITCZ) (Nicholson, 2018; Nicholson and Dezfuli, 2013). The latter one (SON) during the boreal autumn is stronger, following the lengthening and widely spreading dry boreal summer (Jiang et al., 2019), and is associated with a different dynamical mechanism than that of the MAM rainy season (Jackson et al., 2009). Mid-level African Easterly jets (AEJ), especially the southern hemispheric branch (AEJ-S), are known to play a crucial role in the boreal autumn wet season (Adebiyi and Zuidema, 2016; Jackson et al., 2009; Nicholson and Grist, 2003). The AEJ-S is associated with equatorward convergence (Adebiyi and Zuidema, 2016) and is strong during the boreal autumn season, but absent during the boreal spring or MAM season (Adebiyi and Zuidema, 2016; Jackson et al., 2009). Very intense mesoscale convective systems (MCS) are associated with the presence of the AEJ-S and bring rainfall during boreal autumn (Jackson et al., 2009; Vondou et al., 2010). Thus, the AEJ-S timing and strength might play an important role in accelerating or delaying the wet season onset over the Congo basin.

Year	Onset Pentad	Day	Month
2003	59	295	Late-October
2004	51	255	Mid-September
2005	51	255	Mid-September
2006	56	280	Early-October
2007	48	240	Late -August
2008	53	265	Late-September
2009	54	270	Late-September
2010	56	280	Early-October
2011	50	250	Early-September
2012	48	250	Early-September
Solstice	35	171	June 20
Early: 1-10; Mid: 11-20; Late: 21-31 of a month			

Table 1. Onset pentads between 2003-2012 from GPCP data.

Out of the entire Congo basin, only the Angolan coast in the west and the eastern Zaire basin are regulated by the sea surface temperature (SST) anomalies. Circulation features associated with El Nino (La Nina) conditions are strongly linked to wet (dry) conditions over the eastern Zaire basin. Warmer western Indian Ocean SST is somewhat weakly associated with the rainfall over there compared to a strong association between the Atlantic SST and the rainfall over the Angolan Coast (Dezfuli and Nicholson, 2013). Since rainfall onsets in the late August to early September during the early onset years (Table 1), we plot tropical δSST (differences in SST between early- and late-onset years and henceforth for other parameters) during August and September in Fig. 1 from AIRS datasets. Fig. 1 shows that although SST over the Indian Ocean is higher, La Nina condition prevails over the Pacific Ocean during the early onset years. On the other hand, La Nina conditions, warm SST along the Benguela coast, colder western Indian Ocean are related to the wet conditions over the Angolan coast (Dezfuli and Nicholson, 2013). The rainfall variability over the Angolan coast exhibits the strongest correlation (r=0.74) with the SST differences between the warmer Benguela current (10°E–coast, 2°–16°S) and colder western equatorial Indian Oceans (coast–56°E, and 2°–14°S) (Dezfuli and Nicholson, 2013). Although La Nina condition develops and Benguela current is warmer, SST over the western equatorial Indian ocean is higher in August-September (Fig. 1) during the early onset years. As a result, SST differences between the western equatorial Indian Ocean and Benguela current decreases. Other regions over the Congo basin, such as the northern and southern areas of the Zaire basin, northern slopes of the Central African plateau, highlands of the central African Republic show weak relationships with the circulation features, sea level pressure, and SST (Dezfuli and Nicholson, 2013; Vondou et al., 2010). Rather, the rainfall variability over the central Congo basin (15°-25°E) is strongly associated with the stronger easterly tropical jet and local effects (Adebiyi and Zuidema, 2016; Dezfuli and Nicholson, 2013; Jackson et al., 2009; Nicholson and Grist, 2003; Vondou et al., 2010). Thus, these results explain that the SST patterns cannot solely explain the early arrival of the wet conditions over the Congo rainforest.

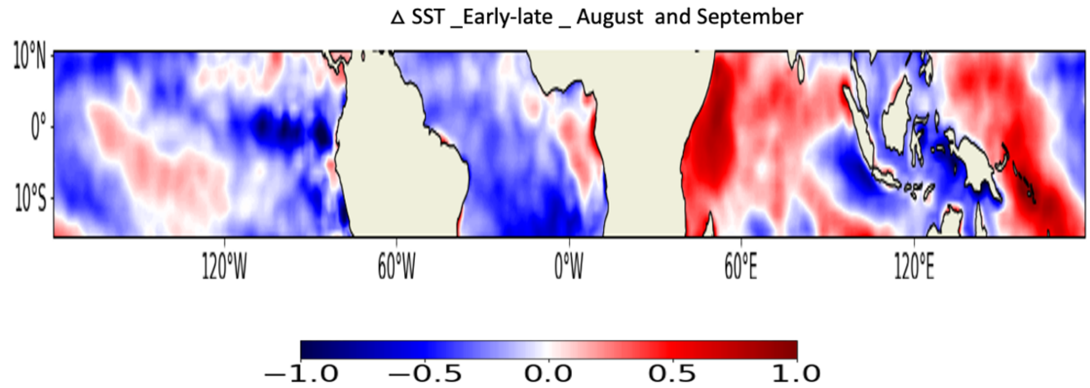

Figure 1. Map of mean of August and September δSST for between the early and late-onset years.

The moisture source during the wet season is the low-level westerly jet that brings moisture from the Atlantic Ocean below 850 hPa (Cook and Vizy, 2016; Neupane, 2016; Nicholson, 2018); however, we observe that the difference in the atmospheric moisture content (not shown) is insignificant between the early- and late-onset years (Dezfuli and Nicholson, 2013). Thus, over a large part of the rainforest, as indicated by many studies in the past (Adebiyi and Zuidema, 2016; Dezfuli and Nicholson, 2013; Jackson et al., 2009; Nicholson and Grist, 2003), zonal circulation and stronger tropical easterly jets might explain the rainfall variability and onset timing. Hence, we focus on the influence of the regional thermodynamic and dynamical conditions on the wet season onset over the Congo basin as suggested by previous studies (Jackson et al., 2009; Vondou et al., 2010).

On the other hand, it is known that dust aerosols are abundant with frequent outbreaks over the Congo rainforest (Laurent et al., 2008) and they can modulate the precipitation over Africa (N’Datchoh et al., 2018). Aerosols have a radiative cooling impact at the surface because they reflect, scatter, and absorb sunlight (Léon et al., 2002). Such a cooling effect can influence the meridional temperature gradient, which is the primary driver of the thermally driven jets. A few attempts, mostly using model simulations, have been made to tease out the dust impacts on the west African monsoon (Lavaysse et al., 2011; Marcella and Eltahir, 2014); however, such studies over the Congo rainforest are absent. Adebiyi and Zuidema (2016) found out that a high amount of aerosol concentration (aerosol optical depth, AOD>0.5) coexists with the SAE-J. However, till date, it is not clear whether aerosols can influence the wet season onset timing over the Congo rainforest despite their well-known impact on the downward shortwave radiation over the rainforest (Konzelmann et al., 1996), and the impact of the meridional temperature gradient between the Congo rainforest and the Kalahari Desert on the AEJ-S (Adebiyi and Zuidema, 2016; Cook, 1999).

Improved understanding of the mechanisms that affect the timing of the wet season is important for an accurate representation of the wet season onset in climate models (Whittleston et al., 2017), for reducing the large uncertainty in the rainfall variability over the Congo rainforest (Whittleston et al., 2017), and assessing the future and sustainability of the rainforest under various global warming scenarios. The Congo rainforest has been far less studied compared to the Amazon rainforest (Wright et al., 2017). Although it is known that the AEJ-S is central to the boreal autumn wet season over the Congo rainforest, the reasons behind the early or late wet season onset are not clear. In particular, it is not clear whether and how aerosol loading, in addition to the meteorological, radiative, and dynamic parameters, affect the timing of the wet season onset.

In this study, we examine the wet season onset timing mechanism by analyzing the aerosol radiative effect on surface temperature (Ts), AEJ-S, and associated convergence. We use a suite of satellite measurements, ERA-Interim and Modern Era Retrospective-Analysis for Research and Applications (MERRA2) dataset over 10 years (2003-2012), focusing on the domain of 5ºN-10ºS,12ºE-32ºE to tease out the influence of the aerosol radiative effect on the wet season onset.

What changes in the meteorological, dynamical, and aerosol concentration lead to an early onset in some years, but a delayed onset in other years? To understand what causes the differences in the wet season onset, we compare the differences in the above-mentioned conditions between three early-onset (2007, 2011, and 2012) and three late-onset (2003, 2006, and 2010) years (Table 1). Methods to calculate the onset pentads from the Global Precipitation Climatology Project (GPCP) data are given in the methodology section. We calculate precipitation variability between the early- and late- years from GPCP data. We use cloud cover and surface irradiance data from the Cloud and the Earth's Radiant Energy System (CERES). The AOD data from the Moderate Resolution Imaging Spectroradiometer (MODIS) is used. Ts is obtained from the Atmospheric Infrared Sounder (AIRS) and ERA-interim reanalysis is used to detect the AEJ-S and calculate divergence (see Supporting Material).

2. Data and methodology

2.1 Data

GPCP pentad data

The Global Precipitation Climatology Project (GPCP) pentad rainfall data have been used to compute the climatological mean and the wet season onset dates. The data are provided in a 2.5° resolution at a 5-day (pentad) temporal average and available at https://data.nodc.noaa.gov/cgi-bin/iso?id=gov.noaa.ncdc:C00933. The version 2.2 data set has rainfall records from 1979 to present. GPCP pentad data have been used for wet season onset related analysis in previous studies (Li and Fu, 2006; Wright et al., 2017).

Cloud and the Earth's Radiant Energy System (CERES)

CERES provides cloud cover and radiant information at 1° spatial resolution at daily scale. We use the SYN1deg data set (https://ceres.larc.nasa.gov/products.php?product=SYN1deg) for this study. The product uses 3 hourly radiances and cloud properties to provide cloud cover, surface radiance, 500 hPa radiance values. We use the longwave and shortwave data at both the upward as well as downward direction in the all-sky and clear-sky conditions. CERES data have previously been used in wet season onset related studies (Wright et al., 2017) are well-validated against the in-situ measurements (Loeb et al., 2018).

Moderate Resolution Imaging Spectroradiometer (MODIS)

We use MODIS daily aerosol products to calculate daily aerosol optical depth (AOD) over the domain. MODIS provides AOD over the oceans and land at a spatial resolution of 10 x 10, 1 km pixels. The MODIS onboard the Aqua satellite data are available every day from 2002 (https://ladsweb.modaps.eosdis.nasa.gov/missions-and-measurements/science-domain/aerosol) and have been extensively used for scientific purposes in the past few decades (Adebiyi and Zuidema, 2016; Fan et al., 2016). MODIS AOD has been used by many researchers to study aerosol-cloud interaction (Gryspeerdt et al., 2015), aerosols radiative impact (Adebiyi and Zuidema, 2016), the relationship between $PM_{2.5}$ concentration and human health (Owili et al., 2017) over the Congo basin. Over the Central Africa, MODIS AOD retrievals with high data quality flag from Terra and Aqua platforms are found to have high correlation (0.87) with the AERONET station data (Gupta et al., 2018).

Atmospheric Infrared Sounder (AIRS)

AIRS data are available from 08-21-2002 (https://disc.gsfc.nasa.gov/datasets/AIRX3STD_006/summary?keywords=airs%20version%206) with a spatial coverage of 180°E to 180°W and 90°S to 90°N. We use the AIRS in combination with Advanced Microwave Sounding Unit (AMSU) and the Humidity Sounder for Brazil (HSB) data. These data use visible, infrared, and microwave sensors to estimate water vapor and 2m surface temperature. AIRS is an instrument onboard the Aqua satellite, which is a part of the A-Train constellation. We use the AIRX3STD (Susskind et al., 2014) daily version 6 standard physical retrieval data at 1° horizontal resolution.

ERA-Interim

We use ERAi data that are available from 1979 to August 2019. We use the zonal and meridional wind data to analyze the wind field and the jet location for our study. Previous studies have already used ERAi data to detect the African jets (Cook, 1999; Jackson et al., 2009). The data are available at a 0.75 x 0.67 spatial resolution in the longitudinal and latitudinal direction, respectively at four different hours (00, 06, 12, 18) of temporal resolution. The data are available at 60 pressure levels from the surface to 0.1 hPa, which can be found at https://www.ecmwf.int/en/forecasts/documentation-and-support/60-model-levels. We have used 673 hPa and 897 hPa levels wind data to calculate the intensity and direction of the Southern as well as Northern African Easterly jets (AEJ-S and AEJ-N) and low level African westerly jet, respectively.

Modern Era Retrospective-Analysis for Research and Applications (MERRA2)

We use two-dimensional hourly averaged surface and vertically integrated aerosol mass fluxes (tavg1_2d_aer_Nx) from the Modern Era Retrospective-Analysis for Research and Applications (MERRA2) data sets (Gelaro et al., 2017). The gridded data are provided in 576 grids along the longitudinal and 361 grids along the latitudinal direction. To understand the aerosol transport over the region, we use the Modern-Era Retrospective analysis for Research and Applications (MERRA-2) aerosol reanalysis (Gelaro et al., 2017) dataset. The MERRA-2 aerosol mass flux data have been widely used to for aerosol transport-related studies (Sitnov et al., 2020; Xu et al., 2020) including the ones that detect and identify aerosol atmospheric rivers as well as major aerosol transport pathways across the globe (Chakraborty et al., 2021). The dataset provides us an opportunity to detect the sources and pathways of aerosols particles transported over the Congo rainforest. The MERRA-2 aerosol reanalysis data are validated against 793 Aerosol Robotic Network (AERONET) stations (Gueymard and Yang, 2020) and has already been used for scientific purposes (Sitnov et al., 2020; Xu et al., 2020). The data provide five different aerosol mass fluxes, such as dust (DU), organic carbon (OC), black carbon (BC), sulfates (SU), and sea salt (SS) in the zonal and meridional direction. We use this dataset to estimate the dominant aerosol types that contribute to the largest fraction to the aerosol concentrations. MERRA provides vertically integrated aerosol mass flux in each grid cell in the zonal (AMFu) and the meridional directions (AMFv) as $\frac{1}{g}\int_{sfc}^{TOA}(A.U)dp$ where p is pressure, A is aerosols mass mixing ratio, U is wind vector, and g is the gravitational constant. We compute integrated aerosol mass flux as $\sqrt[2]{AMFu^2 + AMFv^2}$.

2.2 Methods

We first compute mean rainfall over the domain (5ºN-10ºS,12ºE-32ºE) from 1979 for each pentad. GPCP Pentad data have often been used to detect wet season onset over other regions of the world (Li and Fu, 2006; Wright et al., 2017). The climatological (1979-2013) mean rainfall is 4.14 mm/day over the domain. We detect onset dates each year based on three criteria: 1) the rainfall of that pentad is higher than the climatological mean, 2) five out of eight pentads before that pentad has rainfall less than the climatological mean, and 3) five out of eight pentads after that pentad has rainfall more than the climatological mean (Wright et al., 2017). Onset pentads between 2003-2012 are shown in Table 1. We used GPCP daily data to compute five days (pentad) rainfall. We compute rainfall time series during the three early (2007, 2011, 2012) and three late

(2003,2006, 2010) in Fig. 1A. The differences in rainfall and other parameters including cloud cover, AOD, wind speed of the AEJ-S, and radiation fluxes from June to September between the early- and late-onset years are computed.

We compute cloud cover from CERES and AOD from MODIS datasets. We compute pentad values of low, mid-low, mid-high, and high cloud cover (%) over the domain. To compute AOD, we used daily Aqua MODIS AOD data and averaged over five consecutive days to estimate pentad AOD values over the domain. To understand the relationships between rainfall onset and meteorological as well as dynamical conditions over the domain, we have computed various other parameters from various satellites and ERA-interim reanalysis datasets. We compute net downward shortwave energy (SWnet) as a difference between the downward shortwave energy and upward shortwave energy at the surface from CERES data.

We use daily AIRS 2m surface temperature (Ts) to calculate the pentad values over the domain. To detect the African Easterly Jets, we use ERA interim zonal and meridional wind data. For the Southern African Easterly Jet (AEJ-S), we use the 650 hPa between 5º-15ºS and 12º-24º E (Adebiyi and Zuidema, 2016). We show the wind map of the jet over the domain in Figure 3. We also use wind speed and direction in our analysis to show the maps of the easterly jets at 650 hPa. To compute divergence, we have used the divergence equation as:

$$div = \frac{du}{dx} + \frac{dv}{dy}$$

Where u and v are the zonal and meridional wind and x and y are the longitudinal and latitudinal distances, respectively.

3. Results

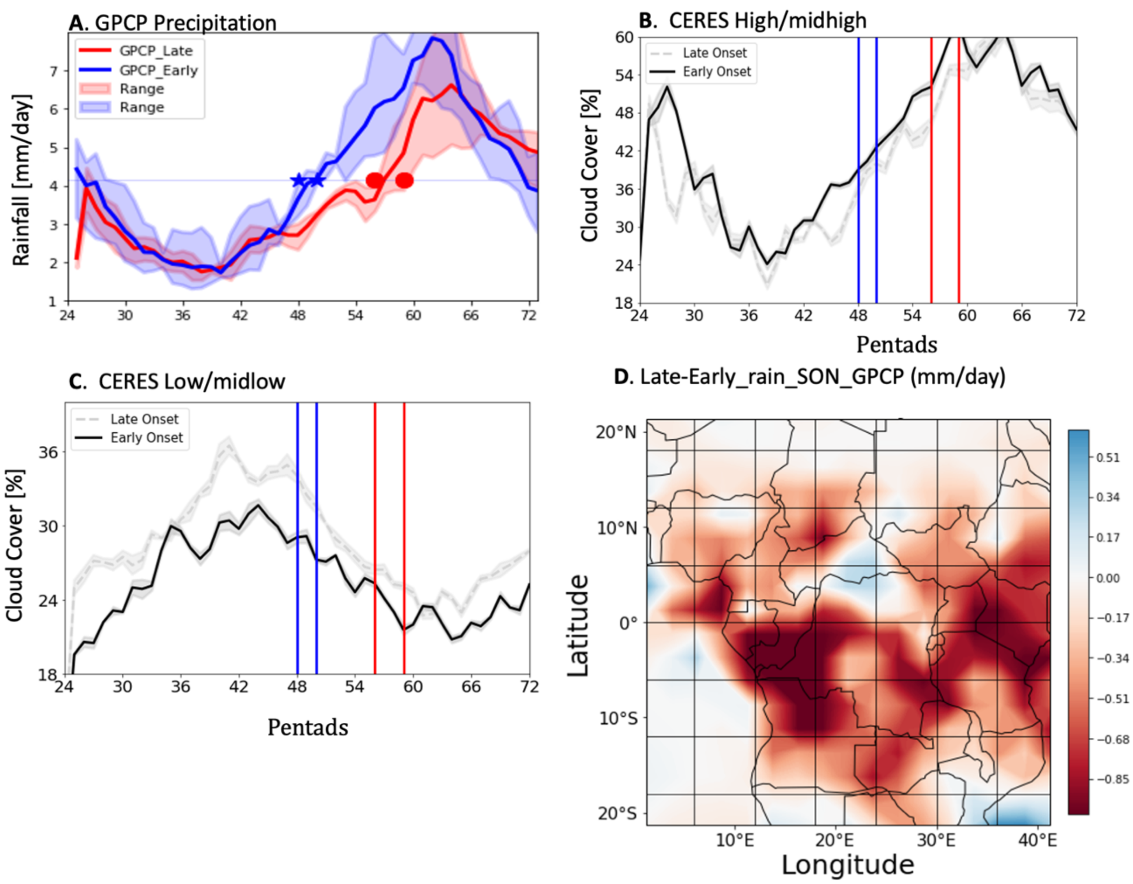

Figure 2. (A) Mean precipitation time series during the early (blue) and late (red) onset years at each pentad. Blue stars (red circles) represent the timing of the early (late) onset years. Rainfall ranges represent precipitation of individual late- or late-onset years. Mean high and mid-high cloud cover **(B)** and low and mid-low cloud cover **(C)** during the early and late-onset years. Vertical lines show the ranges of onset times during the early (blue) and late (red) years. **(D)** Maps of precipitation differences between the late and early-onset years using GPCP data. The shading indicates two sigma errors.

Figure 2A shows a time series of precipitation over the domain during the early and late-onset years. Precipitation (Fig. 2A) and high cloud cover (Fig. 2B) increases during August (42-48th pentads) when the wet season is early (blue stars, Fig. 2A) compared to their slower pick-up during the late-onset years (red circles, Fig. 2A). The wet season starts in late August to early September during the early onset years, unlike the late-onset years when the onset delays until October (Table 1). The rainforest also receives less rain (~ 1 mm/day) during the late-onset years (Fig. 2D). However, low cloud cover is larger during the late onset years after the 38th pentad as compared to the early-onset years (up to 11%, Fig. 2C). Although low clouds can also induce surface cooling, our results show the low cloud cover is higher during the late onset years when the rainforest surface is warmer than the early onset years. The reason why we don't observe the cooling effect from the low clouds on surface cooling could be related to the fact that the low cloud fraction is large over the Angolan coast (~70%), but sharply decreases in land. Low cloud cover is below 15% east of 12°E during June-September (pentads 30-54) (Dommo et al., 2018).

Figures 3A-3D show the differences in the δTs (shaded contours,) and the 650 hPa wind speed (arrows, δWind) and wind direction over the domain between the early- and late-onset years from June to August. They show that the Congo rainforest is cooler by more than 3K in June-August prior to the early-onsets. Such a cooling creates an early and stronger meridional temperature gradient throughout boreal summer before the wet season starts during the early onset years. As a result, δWind at 650 hPa is easterly as early as in June between 8°S -16°S (Fig. 3A). The wind speed difference between the early and late-onset years is significant (>3m/s) with respect to the climatological mean speed of ~7 m/s (Adebiyi and Zuidema, 2016). The wind is westerly during the late onset years in June (Fig.S2), but is easterly during early inset years below 10°S where the SEA-J is generally known to form (Adebiyi and Zuidema, 2016). The AEJ-S is known to form over the Southern hemisphere and gradually move towards the equator as the wet season approaches. In July (Fig 3B), the easterly δwind spreads over most of the domain. Stronger easterly wind is also noted in July-September (Fig. S2). δWind is cyclonic in the Southern hemisphere in August (Fig. 3C) and over the Congo rainforest in September (Fig. 3D) during the early-onset years compared to the late-onset years. Consequently, Figure 5 shows that the southern hemisphere is more convergent during the early-onset years. As a result, high cloud cover (Fig. 2B) and precipitation (Fig. 2A) increase from August and wet season onsets as precipitation gradually increases. These findings suggest that stronger surface cooling and earlier formation of the AEJ-S lead to an earlier wet season onset. The differences in Ts between the early and late onset years is also observed when we plot the actual temperature (Fig. S1). A slightly higher temperature is observed in the bottom row (late onset years). It should be noted that in June-July, the Sun is in the northern Hemisphere. Thus, a slight difference in the temperature due to the aerosols in the southern hemisphere can lead to the formation the AEJ-S.

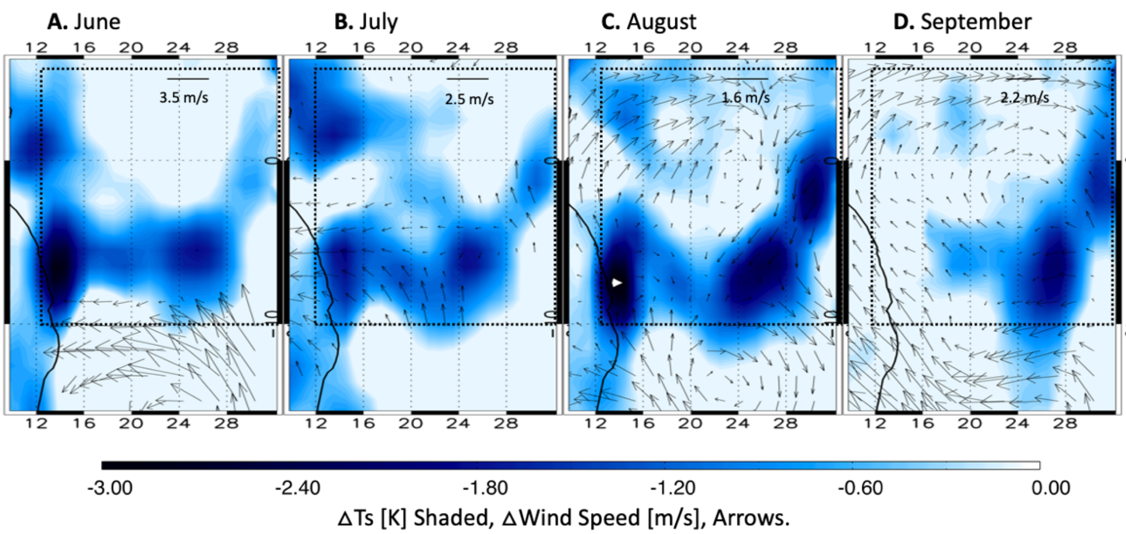

Figure 3. Map of differences in 2m skin temperature (δTs, shaded contours) from AIRS and 650 hPa δwind (arrows) from ERA-interim between **(A)** 30^{th}-36^{th} pentads or June, **(B)** 36^{th}-42^{nd} pentads or July, **(C)** 42^{nd}-48^{th} pentads or August, and **(D)** 48^{th} -54^{th} pentads or September between three early-onset years (2007, 2011, and 2012) and three late-onset years (2003, 2006, 2010). Only the easterly winds are shown in **(A)** and **(B)** to show the location of AEJ-S.

Figure 4 shows the differences in various parameters related to the wet season onset between the early- and late-onset years. Figure 4A shows that δAOD is positive during the early-onset years from the 28^{th} pentad (late May). The accumulation of aerosols in the early-onset years is higher during the 30^{th}-39^{th} pentads and continues until the 45^{th} pentad. The surface during the early-onset years is cooler (Fig. 4B) than the late-onset years, with the strongest cooling coinciding to (domain mean δTs ~-0.7° K) with the higher δAOD during the 30-38^{th} pentads in

June-mid July. All-sky δSWnet is less (Fig. 4C) compared to the late-onset years. The reduced all-sky δSWnet can be attributed to higher δAOD (Fig. 4A) during the 30-38th pentads as cloud cover difference is insignificant (Figs. 2B and C) during that time. The role of AOD on the surface cooling is confirmed in Figure 4D, which shows that the clear-sky δSW_{net} reaches up to -10 W/m^2 during the 30-38th pentads. A strong negative correlation exists between the clear-sky

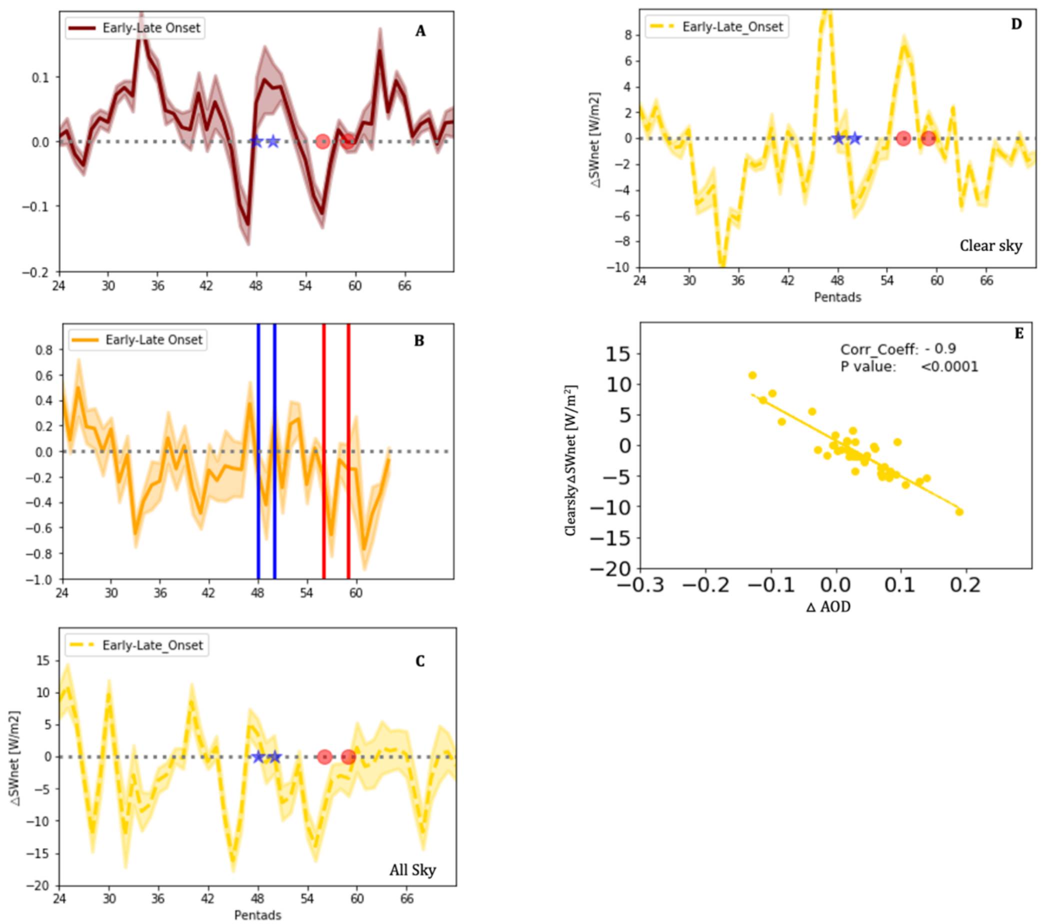

Figure 4. (A) Differences in MODIS AOD (δAOD) from the 24th (day 120) pentad to 72nd pentad (day 360), **(B)** As in A, but for δTs from AIRS. Values up to 66th pentad are shown due to data unavailability in some days after the 66th pentad, **(C)** as in A, all-sky net downward shortwave energy difference at the surface (δSWnet) from CERES, **(D)** As in A, but for clear-sky net downward shortwave energy difference at surface (δSWnet) between the early and late-onset years from CERES. **(E)** Correlation between δAOD difference (in Fig. 3A) and clear-sky δSWnet (in Fig. 3D) between the early and late-onset years at the surface**.** The shading shows two sigma errors.

δSW_{net} and δAOD during the 30-48 pentads (r=-0.9, Fig. 4E), suggesting that aerosols play a significant role in reducing the SW_{net} over the rainforest during the early-onset years. A lower all-sky and clear-sky δSW_{net} give rise to a lower δTs. Hence, these results suggest that aerosols have a strong impact on the timing and strength of the AEJ-S by reducing SWnet at the surface and Ts over the Congo rainforest. Such a cooling begins as early as in June and continues throughout the summer during the early onset years.

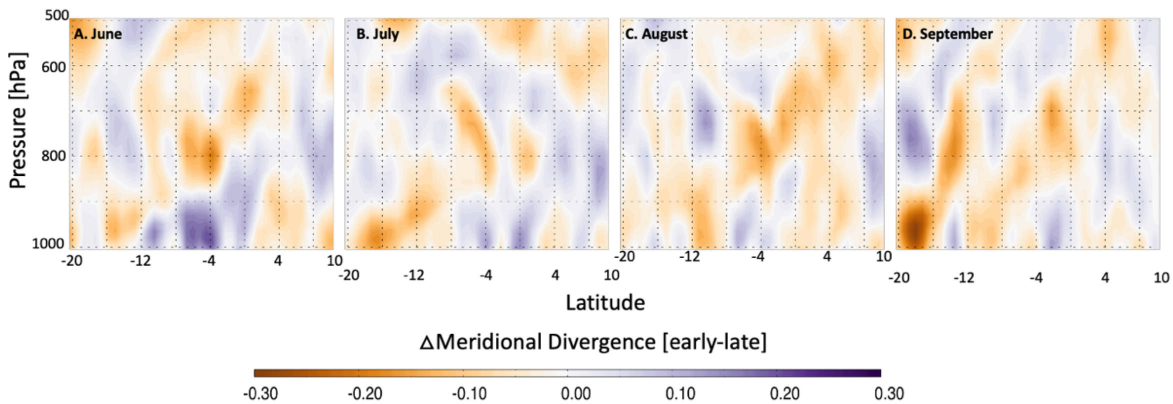

Figure 5. Differences in the mean meridional divergence between 10N to 20S between 1000 hPa to 500 hPa (Y axis) averaged over 12°E-32°E over between the early- and late-onset years during **(A)** 30^{th}-36^{th} pentads or June, **(B)** 36^{th}-42^{nd} pentads or July, **(C)** 42^{nd}-48^{th} pentads or August, and **(D)** 48^{th} -54^{th} pentads or September.

Several important changes in the cloud cover, SW_{net}, precipitation, and AOD occur after the 40^{th} pentad during the early onset years. An early formation of AEJ-S and stronger easterly wind makes the southern hemisphere more convergent (Figs. 5). The domain (5°N-10°S) experiences a comparatively stronger convergence from August. Thus, high cloud cover (Fig. 2B) and precipitation (Fig. 2A) increase between the 42^{nd}-48^{th} pentads during the early-onset years as compared to late-onset years. δAOD also increases between the 40^{th} -45^{th} pentad (Fig. 4A). As a result, clear-sky δSW_{net} reduces by 5W/m^2 during 40-45 pentads (Fig. 4D), whereas all-sky δSW_{net} reduces by 18W/m^2 during 43-47 pentads (Fig. 4C) because of higher high cloud cover

(Fig.2B). Although clear-sky δSW_{net} increases by (Gelaro et al., 2017)~10W/ m^2 during 45-48 pentads as δAOD decreases due to higher precipitation and high/midhigh cloud cover, all-sky δSW_{net} only increases by 5 W/m^2 after the 47th pentad. Hence, δTs decreases by up to 3K in August (Fig. 3C). Mean δTs over the domain decreases by 0.2-0.5K (Fig. 4B) between 40-46th pentads. These results point out that aerosol induced cooling in early boreal summer (June-mid July) leads to higher cloud cover and precipitation in the late summer by influencing the timing and strength of AEJ-S and associated convergence. Such changes in cloud cover in the late summer play a significant role on the all-sky δSW_{net} and the domain Ts during the late summer (August). As a result, the onset timing is highly correlated with the AOD over the domain. The correlation (r) between the onset dates and the AOD averaged over June-August (Fig. 6) is -0.57 (blue dots and line; p value = 0.085). When June AOD is correlated with the onset dates, correlation coefficient becomes even stronger (red dots and line; r = -0.72, p value = 0.02). These results indicate a close relationship between the dry period AOD and the wet season timing over the Congo basin.

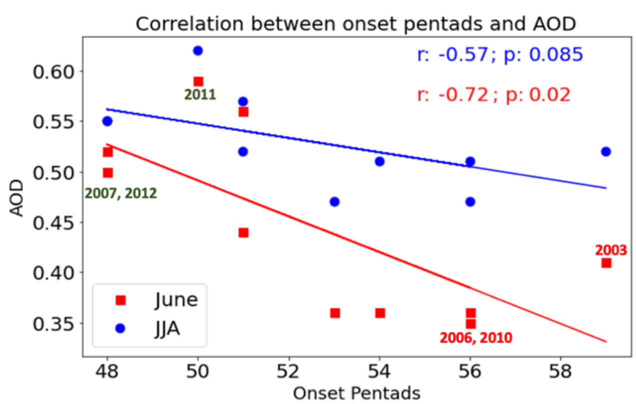

Figure 6. Correlation between the domain mean AOD between June-August and June with the onset pentads. There early and late onset years have also been marked.

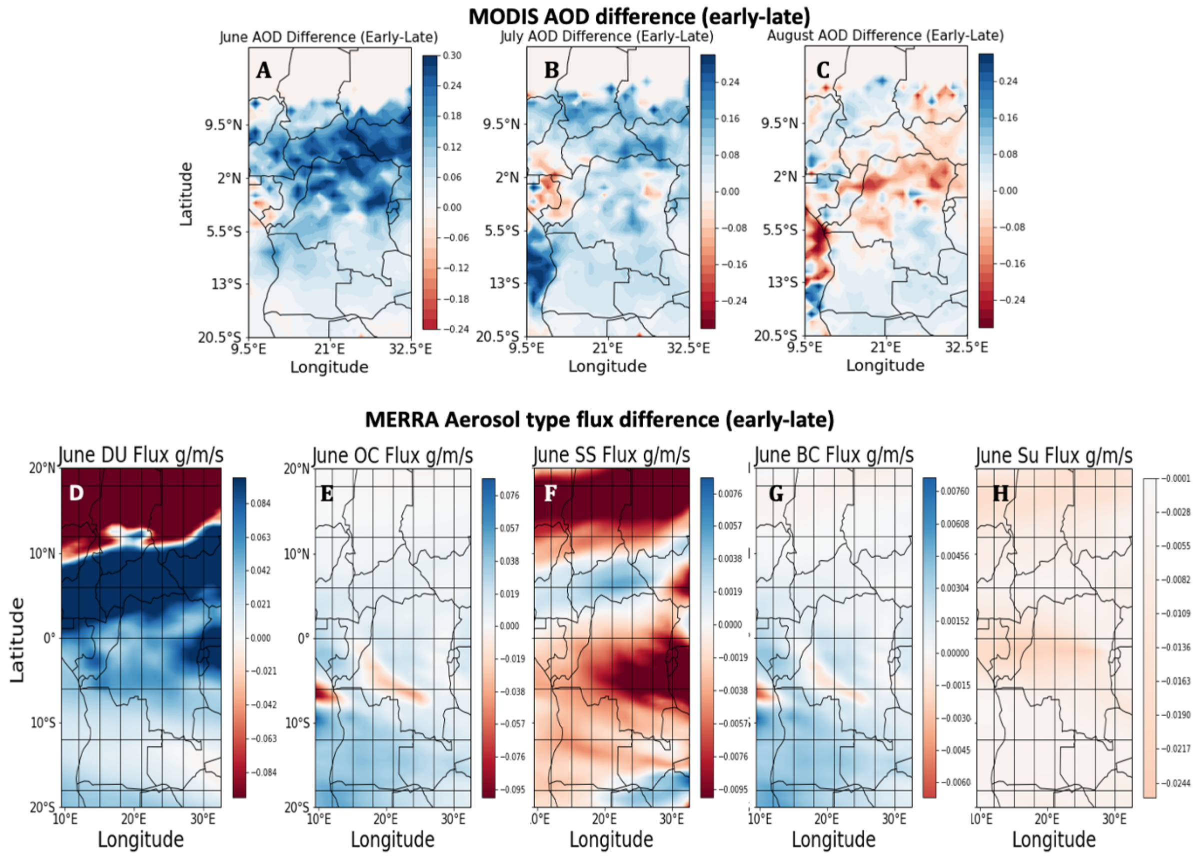

Figure 7. Maps of MODIS AOD difference (δAOD) between the early and late-onset years in **(A)** June, **(B)** July, and **(C)** August. Differences in MERRA2 integrated aerosol mass flux for five different species **(D)** dust, **(E)** organic carbon, **(F)** sea salt, **(G)**, black carbon and **(H)** sulfate between the early and late-onset years during June.

Maps of δAOD from MODIS data are shown in Figs. 7A-C that confirm that the largest difference in AOD is seen in June when δTs is the highest and the AEJ-S begins (Fig.3A). We further analyze the integrated aerosol mass flux datasets from MERRA2 reanalysis products to understand what species of aerosols dominate the higher aerosol loading over the rainforest in June. Our analysis show that a reasonable agreement between MODIS June AOD (Fig. 7A) and MERRA2 dust mass flux (Fig. 7D). The differences in AOD between the early- and late-onset years is primarily due to the changes in the dust concentrations (Fig. 7D) based on the MERRA2 integrated aerosol mass flux data sets (Randles et al., 2017). The cause of the dust appears to be the long-range transport from the Eastern Saharan Desert and the Arabian Desert along the track of the AEJ-N. These results suggests that the strength and location of AEJ-N might play an important role in the aerosol transport from the Eastern Saharan Desert and the Arabian Desert, thus on the aerosol concentration over the Congo rainforest and associated early wet season onset.

4. Discussion

Schematics in Figure 8 summarize the early- and late-onset mechanism and how aerosols play a vital role in such differences. We highlight the mechanism as follows:

- Higher aerosol concentrations during the early-onset years enhance the reflection and scattering of the incoming solar energy in June. Thus, the rainforest receives a lesser amount of downward shortwave energy.
- Consequently, the Ts decreases and driven by the meridional temperature gradient between the rainforest and the Kalahari Desert, AEJ-S forms early.
- As a result, the region experiences a relatively stronger convergence and the circulation is also relatively cyclonic in the early onset years as compared to the late onset years in June-July. High cloud cover (Fig. 2B) gradually increases and leads to a further reduction in all-sky δSW_{net} and δTs in August. High cloud cover and precipitation (Fig. 2A), which were insignificantly different in June-July, become significantly higher in the early onset years (up to 11%) in August and the wet season onsets in late August to early September.
- As the equatorward convergence increases, a stronger cyclonic circulation develops over the region, high cloud cover increases that lead to a reduction in all-sky δSW_{net} and δTs, the wet season onsets in late August to early September.

- In contrast, aerosol concentrations are less during the late-onset years. Hence, a higher amount of solar energy reaches the surface and the rainforest Ts is higher than the early-onset years. Therefore, the meridional temperature gradient is weaker or becomes negative in the Southern Hemisphere with the Congo rainforest (Kalahari Desert) being warmer (cooler) during the boreal summer (Austral winter, June-August). Consequently, the AEJ-S is delayed, domain experiences weaker convergence and high cloud cover doesn't increase in August as in the early-onset years. In September, as the Sun moves southward, the Kalahari Desert warms up. Compared to the early onset years, a weaker meridional temperature gradient develops across the rainforest and the desert since the rainforest Ts is higher (Fig. 3D) during the late-onset years. As a result, the AEJ-S is weaker. Not only is the wet season delayed and the dry season lengthens, the Congo rainforest also receives lesser precipitation.

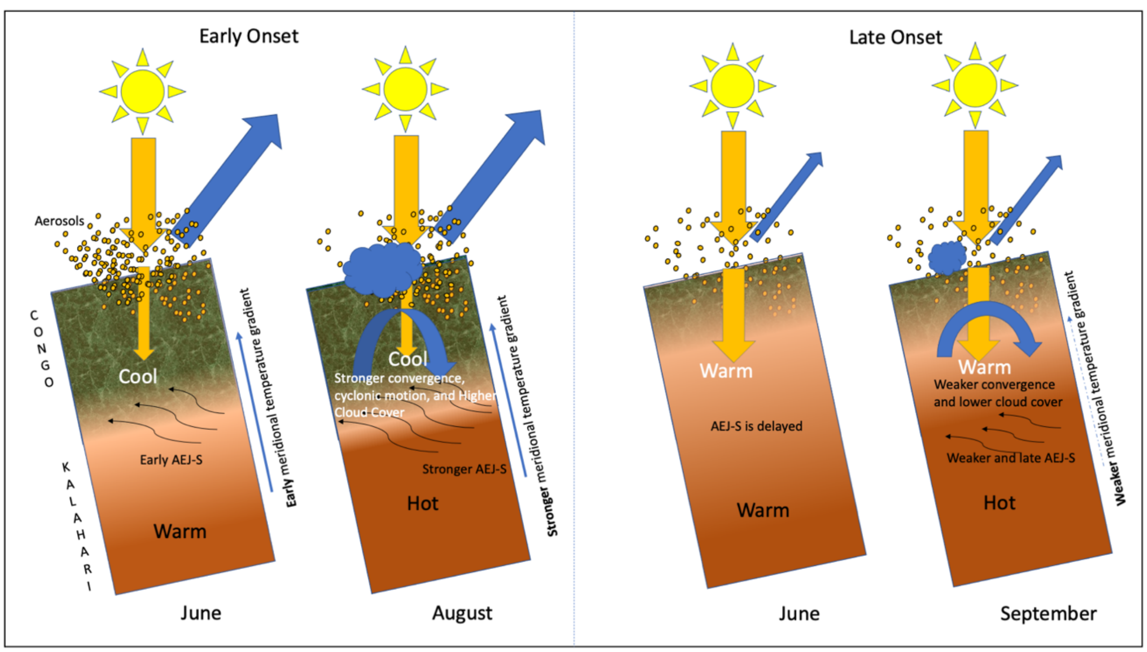

Figure 8. Schematics showing the early- (left) and late- (right) wet season onset mechanism.

5. Conclusion

These above analysis results highlight the interconnections between the aerosols radiative effect and the wet season onset timing by decreasing Ts, increasing meridional temperature gradient, and influencing onset timing and strength of AEJ-S as well as associated convergence. It is important to note that the meridional temperature gradient increases 2-3 months before the wet season onset due to the surface cooling, which is caused by the aerosols dimming effect as the Kalahari Desert is still cold during that time of the year. Because the main driver of the jet is the meridional temperature gradient between the warm/dry Kalahari Desert and the moist Congo rainforest, a reduction in the rainforest Ts (Figs. 3A-D and 4B) in the summer leads to an earlier and stronger AEJ-S during the early-onset years. Our results highlight an important connection between the reductions in the clear-sky δSW_{net} in early summer (June-mid July) due to aerosols, all-sky δSW_{net} in the late summer (August) due to a higher cloud cover, and early wet season onset.

These results indicate a plausible significant threat to the future of the Congo rainforest. Between 2003-2012, the regional temperature has increased by 1.1° C and the boreal summer dry season is increasing (Zhou et al., 2014). Thus, a projected increase in the global temperature anywhere between 1.1° to 5.4° C by 2100 (https://www.climate.gov) might be enough to offset a net mean rainforest cooling of ~1°C required (Fig. 4B) for an early wet season onset over the region. This study shows that aerosols may have a significant impact on the wet season onset timing over the Congo Rainforest by reducing the rainforest Ts. However, aerosols may not be the only factor behind the decrease in the rainforest Ts. As seen in Figure 4, change in the rainforest δSW_{net} (Figs. 4C and 4D) is strongly correlated with the δAOD (Fig. 4A); however, the changes in δTs (Fig. 4C) doesn't always follow the changes in δSW_{net} and δAOD and may also depend on the cloud cover. Further studies using model simulations are needed to understand the relative contribution of aerosols on the wet season onset to separate the roles of other meteorological and dynamical parameters that might also cause the reduction in Ts.

Our analysis using MERRA2 reanalysis data indicates that the location and strength of the AEJ-N and the tropical easterly jet might play an important role in the AOD variation (Fig. 7). However, further analysis is required to tease out the role of these jets and their interannual variability on the dust mass flux and wet season onset. MERRA2 reanalysis data suggest the possibility of long-range aerosol transport by the AEJ-N. A detailed analysis using satellite as well as ground-based measurements and model simulations can shed more light on the role of dynamics on the aerosol concentration. It is necessary to continue investigating the impacts of global warming, large-scale circulation change, land-use, and canopy cover change due to deforestation on the wet season onset over the Congo rainforest. The microphysical effect of aerosols also needs further study.

Author Contribution:

SC: design the research, analyzed data, wrote the paper.

JHJ: design the research, wrote the paper.

HS: design the research, wrote the paper.

RF: design the research, wrote the paper.

Competing Interests:

The authors have no competing interests.

Acknowledgement

This work was conducted at Jet Propulsion Laboratory, California Institute of Technology, under contract with NASA. This work was partly supported by NASA ROSES CCST Program.

Data and Code Availability

All satellite data used in this study can be downloaded at the EOSDIS Distributed Active Archive Centers (DAACs) at https://earthdata.nasa.gov/eosdis/daacs. Please contact the corresponding author for any questions about how to download the data that are publicly available and codes written in IDL and Python.

References

Adebiyi, A. A. and Zuidema, P.: The role of the southern African easterly jet in modifying the southeast Atlantic aerosol and cloud environments, Q. J. R. Meteorol. Soc., doi:10.1002/qj.2765, 2016.

Chakraborty, S., Guan, B., Waliser, D. E., da Silva, A. M., Uluatam, S. and Hess, P.: Extending the Atmospheric River Concept to Aerosols: Climate and Air Quality Impacts, Geophys. Res. Lett., doi:10.1029/2020GL091827, 2021.

Cook, K. H.: Generation of the African easterly jet and its role in determining West African precipitation, J. Clim., doi:10.1175/1520-0442(1999)012<1165:GOTAEJ>2.0.CO;2, 1999.

Cook, K. H. and Vizy, E. K.: The Congo Basin Walker circulation: dynamics and connections to precipitation, Clim. Dyn., doi:10.1007/s00382-015-2864-y, 2016.

Dezfuli, A. K. and Nicholson, S. E.: The relationship of rainfall variability in western equatorial africa to the tropical oceans and atmospheric circulation. Part II: The boreal autumn, J. Clim., doi:10.1175/JCLI-D-11-00686.1, 2013.

Dommo, A., Philippon, N., Vondou, D. A., Sèze, G. and Eastman, R.: The June-September low cloud cover in Western Central Africa: Mean spatial distribution and diurnal evolution, and associated atmospheric dynamics, J. Clim., doi:10.1175/JCLI-D-17-0082.1, 2018.

Erfanian, A., Wang, G. and Fomenko, L.: Unprecedented drought over tropical South America in 2016: Significantly under-predicted by tropical SST, Sci. Rep., doi:10.1038/s41598-017-05373-2, 2017.

Fan, J., Wang, Y., Rosenfeld, D. and Liu, X.: Review of aerosol-cloud interactions: Mechanisms, significance, and challenges, J. Atmos. Sci., doi:10.1175/JAS-D-16-0037.1, 2016.

Gelaro, R., McCarty, W., Suárez, M. J., Todling, R., Molod, A., Takacs, L., Randles, C. A., Darmenov, A., Bosilovich, M. G., Reichle, R., Wargan, K., Coy, L., Cullather, R., Draper, C., Akella, S., Buchard, V., Conaty, A., da Silva, A. M., Gu, W., Kim, G.-K., Koster, R., Lucchesi, R., Merkova, D., Nielsen, J. E., Partyka, G., Pawson, S., Putman, W., Rienecker, M., Schubert, S. D., Sienkiewicz, M. and Zhao, B.: The Modern-Era Retrospective Analysis for Research and Applications, Version 2 (MERRA-2), J. Clim., 30(14), 5419–5454, doi:10.1175/JCLI-D-16-0758.1, 2017.

Gryspeerdt, E., Stier, P., White, B. A. and Kipling, Z.: Wet scavenging limits the detection of aerosol effects on precipitation, Atmos. Chem. Phys., doi:10.5194/acp-15-7557-2015, 2015.

Gueymard, C. A. and Yang, D.: Worldwide validation of CAMS and MERRA-2 reanalysis aerosol optical depth products using 15 years of AERONET observations, Atmos. Environ., doi:10.1016/j.atmosenv.2019.117216, 2020.

Gupta, P., Remer, L. A., Levy, R. C. and Mattoo, S.: Validation of MODIS 3km land aerosol optical depth from NASA's EOS Terra and Aqua missions, Atmos. Meas. Tech., doi:10.5194/amt-11-3145-2018, 2018.

Jackson, B., Nicholson, S. E. and Klotter, D.: Mesoscale convective systems over western equatorial Africa and their relationship to large-scale circulation, Mon. Weather Rev., doi:10.1175/2008MWR2525.1, 2009.

Jiang, Y., Zhou, L., Tucker, C. J., Raghavendra, A., Hua, W., Liu, Y. Y. and Joiner, J.: Widespread increase of boreal summer dry season length over the Congo rainforest, Nat. Clim. Chang., doi:10.1038/s41558-019-0512-y, 2019.

Konzelmann, T., Cahoon, D. R. and Whitlock, C. H.: Impact of biomass burning in equatorial Africa on the downward surface shortwave irradiance: Observations versus calculations, J. Geophys. Res. Atmos., doi:10.1029/96jd01556, 1996.

Laurent, B., Marticorena, B., Bergametti, G., Léon, J. F. and Mahowald, N. M.: Modeling mineral dust emissions from the Sahara desert using new surface properties and soil database, J. Geophys. Res. Atmos., doi:10.1029/2007JD009484, 2008.

Lavaysse, C., Chaboureau, J. P. and Flamant, C.: Dust impact on the west african heat low in summertime, Q. J. R. Meteorol. Soc., doi:10.1002/qj.844, 2011.

Léon, J. F., Chazette, P., Pelon, J., Dulac, F. and Randriamiarisoa, H.: Aerosol direct radiative impact over the INDOEX area based on passive and active remote sensing, J. Geophys. Res. Atmos., doi:10.1029/2000JD000116, 2002.

Lewis, S. L., Brando, P. M., Phillips, O. L., Van Der Heijden, G. M. F. and Nepstad, D.: The 2010 Amazon drought, Science (80-.)., doi:10.1126/science.1200807, 2011.

Lewis, S. L., Sonké, B., Sunderland, T., Begne, S. K., Lopez-Gonzalez, G., van der Heijden, G. M. F., Phillips, O. L., Affum-Baffoe, K., Baker, T. R., Banin, L., Bastin, J. F., Beeckman, H., Boeckx, P., Bogaert, J., De Cannière, C., Chezeaux, E., Clark, C. J., Collins, M., Djagbletey, G., Djuikouo, M. N. K., Droissart, V., Doucet, J. L., Ewango, C. E. N., Fauset, S., Feldpausch, T. R., Foli, E. G., Gillet, J. F., Hamilton, A. C., Harris, D. J., Hart, T. B., de Haulleville, T., Hladik, A., Hufkens, K., Huygens, D., Jeanmart, P., Jeffery, K. J., Kearsley, E., Leal, M. E., Lloyd, J., Lovett, J. C., Makana, J. R., Malhi, Y., Marshall, A. R., Ojo, L., Peh, K. S. H., Pickavance, G., Poulsen, J. R., Reitsma, J. M., Sheil, D., Simo, M., Steppe, K., Taedoumg, H. E., Talbot, J., Taplin, J. R. D., Taylor, D., Thomas, S. C., Toirambe, B., Verbeeck, H., Vleminckx, J., White, L. J. T., Willcock, S., Woell, H. and Zemagho, L.: Above-ground biomass and structure of 260 African tropical forests, Philos. Trans. R. Soc. B Biol. Sci., doi:10.1098/rstb.2012.0295, 2013.

Li, W. and Fu, R.: Influence of cold air intrusions on the wet season onset over Amazonia, J. Clim., doi:10.1175/JCLI3614.1, 2006.

Loeb, N. G., Doelling, D. R., Wang, H., Su, W., Nguyen, C., Corbett, J. G., Liang, L., Mitrescu, C., Rose, F. G. and Kato, S.: Clouds and the Earth'S Radiant Energy System (CERES) Energy Balanced and Filled (EBAF) top-of-atmosphere (TOA) edition-4.0 data product, J. Clim., doi:10.1175/JCLI-D-17-0208.1, 2018.

Malhi, Y. and Wright, J.: Spatial patterns and recent trends in the climate of tropical rainforest regions, in Philosophical Transactions of the Royal Society B: Biological Sciences., 2004.

Marcella, M. P. and Eltahir, E. A. B.: The role of mineral aerosols in shaping the regional climate of West Africa, J. Geophys. Res., doi:10.1002/2012JD019394, 2014.

Marengo, J. A., Nobre, C. A., Tomasella, J., Oyama, M. D., de Oliveira, G. S., de Oliveira, R., Camargo, H., Alves, L. M. and Brown, I. F.: The drought of Amazonia in 2005, J. Clim., doi:10.1175/2007JCLI1600.1, 2008.

Mayer, A. L. and Khalyani, A. H.: Grass trumps trees with fire, Science (80-.)., doi:10.1126/science.1213908, 2011.

N'Datchoh, E. T., Diallo, I., Konaré, A., Silué, S., Ogunjobi, K. O., Diedhiou, A. and Doumbia, M.: Dust induced changes on the West African summer monsoon features, Int. J. Climatol., 38(1), 452–466, doi:10.1002/joc.5187, 2018.

Neupane, N.: The Congo basin zonal overturning circulation, Adv. Atmos. Sci., doi:10.1007/s00376-015-5190-8, 2016.

Nicholson, S. E.: The ITCZ and the seasonal cycle over equatorial Africa, Bull. Am. Meteorol. Soc., doi:10.1175/BAMS-D-16-0287.1, 2018.

Nicholson, S. E. and Dezfuli, A. K.: The relationship of rainfall variability in western equatorial Africa to the tropical oceans and atmospheric circulation. Part I: The boreal spring, J. Clim., doi:10.1175/JCLI-D-11-00653.1, 2013.

Nicholson, S. E. and Grist, J. P.: The seasonal evolution of the atmospheric circulation over West Africa and equatorial Africa, J. Clim., doi:10.1175/1520-0442(2003)016<1013:TSEOTA>2.0.CO;2, 2003.

Owili, P. O., Lien, W. H., Muga, M. A. and Lin, T. H.: The associations between types of ambient PM2.5 and under-five and maternal mortality in Africa, Int. J. Environ. Res. Public Health, doi:10.3390/ijerph14040359, 2017.

Randles, C. A., da Silva, A. M., Buchard, V., Colarco, P. R., Darmenov, A., Govindaraju, R., Smirnov, A., Holben, B., Ferrare, R., Hair, J., Shinozuka, Y. and Flynn, C. J.: The MERRA-2 aerosol reanalysis, 1980 onward. Part I: System description and data assimilation evaluation, J. Clim., doi:10.1175/JCLI-D-16-0609.1, 2017.

Sitnov, S. A., Mokhov, I. I. and Likhosherstova, A. A.: Exploring large-scale black-carbon air pollution over Northern Eurasia in summer 2016 using MERRA-2 reanalysis data, Atmos. Res., doi:10.1016/j.atmosres.2019.104763, 2020.

Staver, A. C., Archibald, S. and Levin, S. A.: The global extent and determinants of savanna and forest as alternative biome states, Science (80-.)., doi:10.1126/science.1210465, 2011.

Susskind, J., Blaisdell, J. M. and Iredell, L.: Improved methodology for surface and atmospheric soundings, error estimates, and quality control procedures: the atmospheric infrared sounder science team version-6 retrieval algorithm, J. Appl. Remote Sens., doi:10.1117/1.jrs.8.084994, 2014.

Tyukavina, A., Hansen, M. C., Potapov, P., Parker, D., Okpa, C., Stehman, S. V., Kommareddy, I. and Turubanova, S.: Congo Basin forest loss dominated by increasing smallholder clearing, Sci. Adv., doi:10.1126/sciadv.aat2993, 2018.

Vondou, D. A., Nzeukou, A., Lenouo, A. and Mkankam Kamga, F.: Seasonal variations in the diurnal patterns of convection in Cameroon-Nigeria and their neighboring areas, Atmos. Sci. Lett., doi:10.1002/asl.297, 2010.

Whittleston, D., Nicholson, S. E., Schlosser, A. and Entekhabi, D.: Climate models lack jet-rainfall coupling over West Africa, J. Clim., doi:10.1175/JCLI-D-16-0579.1, 2017.

Wright, J. S., Fu, R., Worden, J. R., Chakraborty, S., Clinton, N. E., Risi, C., Sun, Y. and Yin, L.: Rainforest-initiated wet season onset over the southern Amazon, Proc. Natl. Acad. Sci. U. S. A., doi:10.1073/pnas.1621516114, 2017.

Xu, X., Wu, H., Yang, X. and Xie, L.: Distribution and transport characteristics of dust aerosol over Tibetan Plateau and Taklimakan Desert in China using MERRA-2 and CALIPSO data, Atmos. Environ., doi:10.1016/j.atmosenv.2020.117670, 2020.

Zhou, L., Tian, Y., Myneni, R. B., Ciais, P., Saatchi, S., Liu, Y. Y., Piao, S., Chen, H., Vermote, E. F., Song, C. and Hwang, T.: Widespread decline of Congo rainforest greenness in the past decade, Nature, doi:10.1038/nature13265, 2014.